



Performance of nanofiltration and reverse osmosis after membrane bioreactor for urban source-separated urine treatment and water reuse

Mathias Monnot, Bénédicte Nguyen, François Zaviska, Geoffroy Lesage, Marc Héran*

IEM (Institut Européen des Membranes), UMR 5635 (CNRS-ENSCM-UM), Université de Montpellier, Place Eugène Bataillon, F-34095 Montpellier, France, Tel. +33(0)4 67 14 37 23; emails: marc.heran@umontpellier.fr (M. Héran), mathias.monnot@umontpellier.fr (M. Monnot), benedictenguyen@yahoo.fr (B. Nguyen), Tel. +33(0)4 67 14 91 65; email: francois.zaviska@umontpellier.fr (F. Zaviska), Tel. +33(0)4 67 14 33 13; email: geoffroy.lesage@umontpellier.fr (G. Lesage)

Received 25 April 2017; Accepted 13 September 2017

ABSTRACT

In the context of wastewater treatment and reuse, separating urine from domestic wastewater promotes a more flexible and sustainable municipal treatment system and has attracted considerable attention in the scientific community. This study investigated the feasibility of applying nanofiltration (NF) and reverse osmosis (RO) as a complementary treatment after membrane bioreactor (MBR) treatment of source-separated urine. Experiments were conducted on a lab scale with a synthetic effluent containing natural organic matter representative of urine after MBR treatment. The performances of NF and RO in terms of productivity and water quality were compared. NF and RO could remove more than 95% of total organic carbon which is composed mainly of humic and fulvic acids. NF could only reduce the conductivity by less than 45% whereas RO removed more than 80% of ions which would make water reuse more feasible. A complete short-term fouling analysis by membrane autopsy was performed in order to understand the different contributions of organic and inorganic components on NF and RO fouling. The obtained results showed that NF was more prone to scaling as water rinsing and chemical cleaning were not fully effective in removing mineral deposits. RO seemed less prone to organic fouling and scaling than NF.

Keywords: Urine treatment; Wastewater reuse; Nanofiltration; Reverse osmosis; Source separation

1. Introduction

Responding to the increasing water demand, wastewater treatment and reuse is one of the solutions to develop non-conventional water resources [1,2]. Urine source separation is of great interest because most of the nutrients in wastewater (nitrogen and phosphorus) are derived from urine which accounts for less than 1% of the total volume of wastewater [3]. As nitrogen produces toxic effects in rivers and phosphorus produces excessive algal growth, major efforts have been undertaken to precipitate phosphorus and to convert ammonium to gaseous nitrogen. Separating urine from wastewater would offer various advantages such as the reduction of

footprint, energy consumption and improvement of the effluent quality [4]. Therefore, urine source separation could increase the flexibility of wastewater treatment and its treatment for water reuse seems a promising option [5].

Depending on the overall goal of the source-separated urine treatment process, a specific technical solution can be found to meet the requirements [6]. Membrane bioreactors (MBRs) have become a state-of-the-art technology for wastewater treatment [7]. This involves a combination of the conventional biological sludge process with a micro or ultrafiltration membrane system. While the biological process can significantly reduce organic pollutants by biodegradation, the membrane module acts as a physical separation retaining particles and bacteria between the treated water and the mixed liquor. The MBR offers the advantage of low footprint, better water quality and high operational flexibility

* Corresponding author.

(dissociation of the hydraulic retention time to the sludge retention time) [8].

Urine is highly concentrated in different salts (above 10 g/L) and usually represents a chemical oxygen demand to total nitrogen ratio (COD/TN) of below 2 [9]. Fresh urine contains urea that can be hydrolyzed into carbon dioxide and ammonia when it is stored (due to urease activity). Ammonia (NH_3) and ammonium (NH_4^+) are then in equilibrium depending on the pH ($\text{pK}_a = 9.25$). As a result, ammonium ions represent the major compounds of total nitrogen composition of this wastewater influent. The specificity of having a low COD/TN ratio would make the control of MBR operation challenging. Indeed, the low organic carbon load is very favorable to the nitrification stage (as nitrification is carried out by autotrophic bacteria) but may become an obstacle for a full denitrification and impact the total nitrogen removal of treated water [10]. Consequently, there is a risk of accumulating nitrites, NO_2^- or nitrates, NO_3^- [11]. Furthermore, the pH of stored urine is usually around 9 moving the equilibrium toward the NH_3 form which would cause the inhibition of ammonia oxidizing bacteria and thus would hinder the treatment of NH_4^+ increasing even more concentration in NH_3 [9,12,13]. Finally, high concentrations of NH_3 would also cause the inhibition of nitrite-oxidizing bacteria [14].

Due to the possible presence of NH_4^+ , NO_2^- and NO_3^- in the MBR permeate as well as the presence of salts (mainly Na^+ and Cl^-), a complementary treatment after the MBR would thus be needed for complete source-separated urine treatment and possible water reuse. Among the potential post-treatment methods after MBR, the use of nanofiltration (NF) or reverse osmosis (RO) has gained popularity for wastewater treatment and reuse. These pressure-driven processes are set-up in compact systems and can retain ions. Indeed, nanofiltration (NF270 from Dow) after a MBR treating synthetic municipal wastewater could remove 71% of salinity, 84% of total organic carbon (TOC) and 89% of total nitrogen on a lab scale [15]. Kappel et al. [16] studied the combination of MBR and NF with NF concentrate recirculation to the MBR for municipal wastewater treatment and reuse during 1 year. NF270 (Dow) exhibited a rejection of 97% of TOC, less than 40% of monovalent ions (Na^+ and Cl^-), over 60% of Ca^{2+} , Mg^{2+} , Cu^{2+} ions and over 99% of SO_4^{2-} and PO_4^{3-} ions. They demonstrated that NF fouling was not due to the presence of organics but rather due to the presence of inorganics and the major cause of flux decline was due to the precipitation of calcium phosphate.

Jacob et al. [17] compared the performances of NF and RO after a MBR step treating real municipal wastewater. They found that tight NF could reduce over 80% of conductivity and TOC whereas loose NF could only reduce these up to 60%. For tight NF, irreversible fouling occurred at all Transmembrane pressures (TMPs) (4 to 12 bar) due to low molecular weight dissolved organic carbon (DOC). RO could reduce the conductivity and TOC over 90% for any volumetric concentration factor (VCF). Fouling of RO was mainly reversible (over 95% of flux recovery) and due to the rise of the osmotic pressure and non-compressible cake formation.

Lee and Lueptow [18] studied the use of RO to treat spacecraft wastewater containing urea for water reuse. They concluded that even if RO was effective to recover wastewater with high solute rejection, nitrogen rejection increased

significantly after urea hydrolysis, since ammonium ions are more easily rejected by RO membranes. This shows the need for a supplementary process before RO, such as the MBR, to stabilize urine.

However, as previously mentioned, urban source-separated urine would be more concentrated in salts than municipal wastewater and it would be more problematic to reach reuse guidelines for the concentrations of NH_4^+ , NO_2^- and NO_3^- . Moreover, NF and RO foulants may be organic and/or inorganic and, in any case, this seems to be highly dependent on effluent quality.

Consequently, the overall objective of this work was to study the behavior of NF or RO as a post-treatment method after MBR for source-separated urine treatment and reuse. This was done in terms of short-term fouling mechanisms and water quality analysis. In order to reach this goal, synthetic source-separated urine MBR permeate containing natural dissolved organic matter (DOM) was used as a feed for NF and RO on a lab scale. The NF and RO permeate quality was analyzed with special attention given to DOM as well as NH_4^+ , NO_2^- and NO_3^- . The mechanisms of NF and RO membrane fouling were investigated by monitoring TMP, flux decline and recovery and at last by performing a complete membrane autopsy.

2. Material and methods

2.1. Composition of the synthetic MBR permeates from source-separated urine

The mineral composition of the synthetic MBR permeate was based on synthetic nitrified urine composition of Udert and Wächter [19] diluted by a factor of 6 to consider flushing water addition. The assumption of partial nitrification and no denitrification occurring in real MBR fed with source-separated urine was taken into account by adjusting $\text{NO}_2\text{-N}$, $\text{NO}_3\text{-N}$ and $\text{NH}_4\text{-N}$ concentrations. The resulting recipe of the mineral synthetic wastewater is given in Table 1.

Real MBR permeate also contains DOM (typically soluble microbial products and exopolymeric substances). To take into account the influence of DOM, a real MBR effluent from a southern France municipal wastewater treatment plant (80,000 P.E.) was used. This real DOM source was concentrated using RO. Then, dilution was done to get around 10 mg/L of TOC as obtained by Kappel et al. [16]. Obviously, the ionic composition of the resulting effluent also changed accordingly with the concentrations of DOM sources. The average composition of the synthetic effluent with DOM is given in Table 2.

Table 1
Recipe of the mineral synthetic MBR permeate

Chemicals	Concentration (g/L)
NH_4NO_3	0.70
$\text{NaH}_2\text{PO}_4 \cdot \text{H}_2\text{O}$	0.40
KHCO_3	0.95
Na_2SO_4 anhydrous	0.40
NaNO_2	2.30
NH_4Cl	1.40

2.2. RO and NF experimental set-up

NF and RO filtrations were performed using a laboratory-scale cross flow filtration unit (Koch Membrane Systems Labcell-F-1) and under a constant TMP mode. The experimental set-up is illustrated in Fig. 1. The effluent, placed in the feed tank of a maximum capacity of 500 mL, is circulated in cross flow mode thanks to the tangential filtration pump. The temperature of the feed tank was controlled and maintained constant during the experiments thanks to its double envelope and a cooling/heating system. The membrane was mounted on the membrane module and pressurized nitrogen was used to adjust the TMP. The permeate flow rate was

Table 2
Average composition of synthetic MBR permeate

Parameter (mg/L)	MBR permeate with DOM
TOC	10.1 ± 0.2
Inorganic carbon	111 ± 22
Cl ⁻	1,698 ± 14
N-NO ₂ ⁻	424 ± 27
N-NO ₃ ⁻	154 ± 27
SO ₄ ²⁻	456 ± 24
PO ₄ ³⁻	198 ± 29
Na ⁺	1,421 ± 6
N-NH ₄ ⁺	377 ± 36
K ⁺	485 ± 65
Mg ²⁺	56 ± 8
Ca ²⁺	182 ± 74

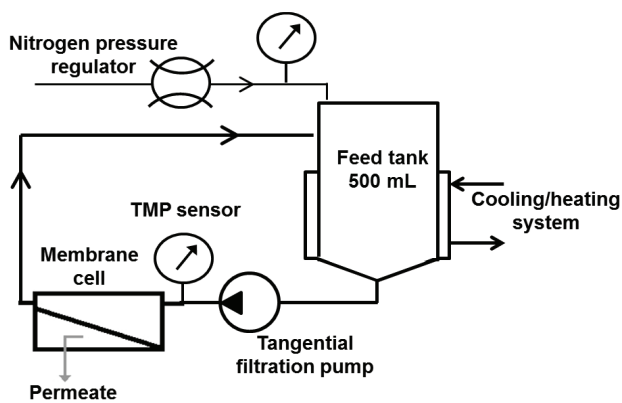


Fig. 1. Illustration of the experimental filtration set-up [20].

Table 3
Characteristics of the NF and RO membranes

	Supplier	Material	pH range	Mean roughness (nm)	Zeta potential (mV) in NaCl, pH > 5
NF 90	Dow Filmtec	Polyamide on	3–10	127 [21]	Negative [21]
TFC-HR	Koch Membrane	polyether sulfone support layer	4–11	64 [22]	Negative [22]

obtained from measurements of permeate mass using an electronic balance.

Two flat sheet membranes with an effective membrane area of 28 cm² were tested: an NF membrane (NF90) and an RO membrane (TFC-HR) whose characteristics are presented in Table 3.

2.3. Filtration method

Experiments were performed by filtrating 300 mL of synthetic mineral MBR effluent or synthetic MBR effluent containing natural DOM (Table 2) at two constant TMPs: 12 or 16 bar. TOC, cation and anion concentrations were measured after the filtration, on the whole collected permeate. A decrease of permeation flux vs. time was observed due to the rise of osmotic pressure, concentration polarization and possible fouling. In order to compare the different experiments with the same matter quantity brought to the membrane surface, it was chosen to present the normalized flux decline as a function of the VCF. The VCF is related to the filtrated volume according to Eq. (1):

$$\text{VCF} = \frac{V_0}{V_0 - V_p} \quad (1)$$

where V_0 is the initial volume in the feed tank (300 mL) and V_p is the volume of permeate. In continuous systems, it is common to use the recovery rate (Y) defined as the ratio between permeate flow rate and feed flow rate. Thus, the recovery rate could be defined according to Eq. (2). Thus, a VCF of 2 could be equivalent to a recovery rate of 50% and a VCF of 3% to 66%.

$$Y = 1 - \frac{1}{\text{VCF}} \quad (2)$$

After conditioning (Milli-Q water soaring and compressing) the new membrane coupons and in order to evaluate membrane fouling, membrane permeability corrected at 20°C was measured with Milli-Q water three times for each experiment: before filtration, after filtration plus rinsing and after chemical cleaning. The correction was made with Eq. (3):

$$Lp_{20^\circ\text{C}} = \frac{\mu_{T^\circ\text{C}}}{\mu_{20^\circ\text{C}}} Lp_{T^\circ\text{C}} \quad (3)$$

To get rid of slight variations in permeability from one membrane coupon to another, permeabilities were normalized by the initial permeability. The water rinsing consisted in removing the membrane from the filtration cell, rinsing it thoroughly with Milli-Q water and then a 10-min Milli-Q water circulation in the filtration cell without permeation

was performed. The chemical cleaning consisted in soaking the membrane for at least 1 h in NaOH solution (0.01 M for NF membranes and 0.001 M for RO membranes according to manufacturers' guidelines) to remove possible organic fouling. Following this, the membrane was rinsed with water and then in HCl solution (0.01 M for NF membranes and 0.001 M for RO membranes to respect manufacturers' guidelines) to remove potential mineral deposits.

2.4. Water quality assessment

The concentration of anions (i.e., Cl⁻, NO₂⁻, NO₃⁻, PO₄³⁻ and SO₄²⁻) and cations (i.e., NH₄⁺, K⁺, Na⁺, Mg²⁺ and Ca²⁺) was measured using an ion chromatograph ICS-1000 (Dionex) equipped with an IonPac AS19 column for the anions and a ICS-900 (Dionex) equipped with a IonPac CS12A column (Dionex) for the cations. Inorganic carbon was measured with a TOC metre (TOC-Vcsh/csn, Shimadzu) and the predominant form was considered to be HCO₃⁻ as the pH of the samples was between 7 and 8. Apparent rejection rates were calculated using Eq. (4) in which C_p is the salt concentration in the permeate and C_f is the salt concentration in the feed:

$$R = 1 - \frac{C_p}{C_f} \quad (4)$$

The TOC concentration was measured with a TOC metre (TOC-Vcsh/csn, Shimadzu) using the non-purgeable organic carbon method, which corresponds to the measurement of DOC, as particulate organic carbon was removed with 1.2 μm syringe filters. Knowing the exact volumes of feed, permeate, rinsing water and concentrate in each experiment, a TOC mass balance was performed to compare the mass of TOC that was initially in the feed to the total mass of TOC collected in the permeate, the rinsing water and the concentrate.

A closer monitoring of the DOC was done thanks to fluorescence measurement. Fluorescence was recorded using a PerkinElmer model LS55 fluorescence spectrophotometer with 1 cm path length quartz cells. Samples were diluted with ultrapure water to avoid any inner filter effect. The dilution ratio was determined after measurements were taken at successive dilution ratios, in order to limit overlapping signals. A fluorescence excitation emission matrix (3DEEM) was obtained by subsequently scanning the emission spectra from 280 to 600 nm and excitation spectra from 200 to 500 nm, both stepped by 10 nm. The fluorescence intensities were corrected by normalising with the Raman spectra of water and subtracting the signal of Milli-Q water. The qualitative analysis of DOM fraction was done thanks to the classification of Chen et al. [23] given in Table 4.

Table 4
Usual classification of fluorescence regions [23]

Fluorescence region	Excitation wavelengths range (nm)	Emission wavelengths range (nm)
Aromatic protein-like fluorophores (Regions I+II)	200–250	280–380
Fulvic acid-like fluorophores (Region III)	200–250	380–600
Soluble microbial product-like fluorophores (Region IV)	250–350	280–380
Humic acid-like fluorophores (Region V)	250–500	380–500

A semi-quantitative method was also attempted here by the integration of the whole fluorescence signal. Hence, the volume of fluorescence (Φ) was calculated from the corrected matrix, following the integration method according to [23] (Eq. (5)):

$$\Phi = \sum_{\text{ex}} \sum_{\text{em}} I(\lambda_{\text{ex}} \lambda_{\text{em}}) \Delta \lambda_{\text{ex}} \Delta \lambda_{\text{em}} \quad (5)$$

in which Δλ_{ex} is the excitation wavelength interval (taken as 10 nm), Δλ_{em} is the emission wavelength interval (taken as 10 nm) and I(λ_{ex}λ_{em}) is the fluorescence intensity at each excitation–emission pair (Raman units).

Similarly to the TOC mass balance, a “volume of fluorescence mass balance” was applied to each experiment assuming that the fluorescence intensity was proportional to the fluorophores concentration.

2.5. Membrane characterization

In order to visualize the membrane surface structure and to identify inorganic deposit, membranes were analyzed with a scanning electron microscope (SEM) (ZEISS EVO 15 HD) with energy dispersive X-ray spectroscopy (EDX) (Oxford AZtec X-Max 50) at 10 kV. For each sample, the EDX measurement was made on several scanning areas selected randomly by the user and the average of the obtained relative mass compositions together with the standard deviation were calculated.

Functional group characteristics of membrane samples were measured by a Thermo Nicolet-6700 Fourier transform infrared (FTIR) spectrometer. The spectra were recorded by the attenuated total reflection (ATR) method with an optic Diamant KRS5. Thirty two scans at a nominal instrument resolution of 4 cm⁻¹ were collected between 500 and 4,000 cm⁻¹. A background spectrum was measured before each measurement for subsequent correction.

To assess hydrophobicity of the membrane surfaces, contact angle measurements of the dried membranes before and after filtration were carried out with a contact angle meter (Automatic Contact Angle Meter, Model CA-VP, Kyowa Interface Science Co., Ltd., Japan) and microscope image processing software (Image J, NIH-freeware version).

3. Results and discussion

3.1. Performances of NF and RO in terms of water quality

3.1.1. Rejection rates

Fig. 1 shows the apparent rejection rates of the main indicators related to permeate quality obtained for NF and RO

filtrations of synthetic urine effluent spiked with DOM at 12 and 16 bar. It is recalled that the analysis of the permeate quality was performed on the whole collected permeate. Considering NF, it could reduce over 95% of TOC for both applied TMP and reduce conductivity by only 30% and 45% at 12 and 16 bar, respectively. Indeed, derived from basic transfer equations, an increase of the effective pressure increased the salt rejection rate in NF or RO [24]. This was verified for all targeted ions as presented in Fig. 2. As also expected, NF rejection was higher for trivalent and divalent ions (more than 96% for SO_4^{2-} and PO_4^{3-} and more than 70% for Mg^{2+} and Ca^{2+}) than for monovalent ions (less than 55%) due to steric effects and electrostatic effects for negatively charged trivalent and divalent ions. Then, a high rejection of SO_4^{2-} and PO_4^{3-} , present in relatively high quantity in comparison with trivalent or divalent cations, may impose a lower rejection of other anions to insure permeate electroneutrality [24] also known as the Donnan effect. Among the studied monovalent anions, NO_3^- and NO_2^- are those with the lowest hydration energy [25] which might explain their low rejection rate (less than 25%). Additionally, the presence of salts at high concentration increased the ionic strength of the solution and thus reduced the membrane zeta potential (the membrane may become less negatively charged here) which may induce a possible shielding effect which could reduce the electrical repulsion between the membrane and the anions.

Regarding RO, the apparent rejection rates, as expected, were systematically higher than those obtained with NF with values higher than 80%. It could also reduce TOC over 95% and conductivity over 90%. Lower rejection rates were also obtained for NO_3^- and NO_2^- , probably because of the same reason as previously propounded for NF.

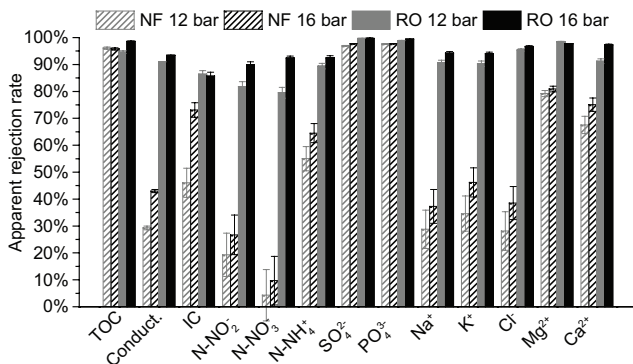


Fig. 2. Apparent rejection rates of NF and RO filtrations at different TMPs with synthetic effluent containing DOM.

Table 5
NF-RO water quality vs. guidelines

	pH	Conductivity (mS/cm)	N-NO ₂ ⁻ (mg/L)	N-NO ₃ ⁻ (mg/L)	N-NH ₄ ⁺ (mg/L)	SO ₄ ²⁻ (mg/L)	Na ⁺ (mg/L)	Cl ⁻ (mg/L)
NF permeate	7.6	6.27	293	111	119	11.2	895	1,037
RO permeate	7.5	0.72	41.9	18.9	30.1	1.37	82.3	56.5
Water reuse guidelines	6.5–8.5	3	30 as total nitrogen		–	–	69	140
Drinking water guidelines	6.5–8.5	0.2–1.1*	0.9	11.0	0.08*	250*	200*	250*

*French drinking water guidelines.

As one of the objectives is to evaluate the feasibility of using NF or RO as a complementary treatment after MBR for water reuse of source-separated urine, Table 5 presents some water quality parameters of the NF and RO permeates obtained at 16 bar. It also enables the comparison with the World Health Organization (WHO) guidelines for wastewater reuse with minor to moderate restriction on agricultural usage [26] and with the WHO or French guidelines (if not given by the WHO) for drinking water quality [27]. It can be seen from this table that the pH of NF and RO permeates follows both guidelines. Only the RO permeate follows the conductivity guidelines. Concerning PO_4^{3-} , K^+ , Mg^{2+} and Ca^{2+} , no specific guideline is provided as they are not of concern for typical concentrations encountered in waters. NF and RO permeates follow both guidelines for SO_4^{2-} and only the RO permeate follows the drinking water guidelines for Na^+ and Cl^- . The water reuse guidelines for agriculture are rather strict. Both permeates are far from the guidelines for NO_2^- , NO_3^- and NH_4^+ . The only way to reduce these nitrogen concentrations is to improve the efficiency of the MBR by improving nitrification and denitrification processes. Nevertheless, depending on the reuse applications, such as for the toilet flush in decentralized systems, RO permeate may be considered appropriate (Table 5).

3.1.2. Organic matter characterization

It was observed previously that NF and RO membranes could retain, probably by steric effects, more than 95% of TOC in the MBR effluent. The following results aim at characterizing the type of DOM. Fig. 3 shows the 3DEEM of NF and RO feeds and permeates for all the experiments. As a matter of clarity, only results obtained at 12 bar are shown but an identical trend was observed at 16 bar. All the feeds mainly present fluorophores in region V (~39% of volume of fluorescence), which are characteristic of humic acid-like substances, in regions III (~21% of volume of fluorescence) which are characteristic of fulvic acid-like and in regions IV (~31% of volume of fluorescence), which are characteristic of soluble microbial product-like substances. Only 10% fluorescence volume was obtained for protein-like substances. This is in agreement with the observations of Jacquin et al. [28]. No fluorescent signal was recorded in almost all permeate samples, meaning that NF and RO retained the totality of fluorescent DOM independently of membrane type and TMP. The 3DEEM of NF and RO concentrates as well as rinsing waters were really similar to those of the feeds. Likewise, their distribution of fluorescence volumes was the same as in the feeds, confirming that all types of fluorescent DOM were

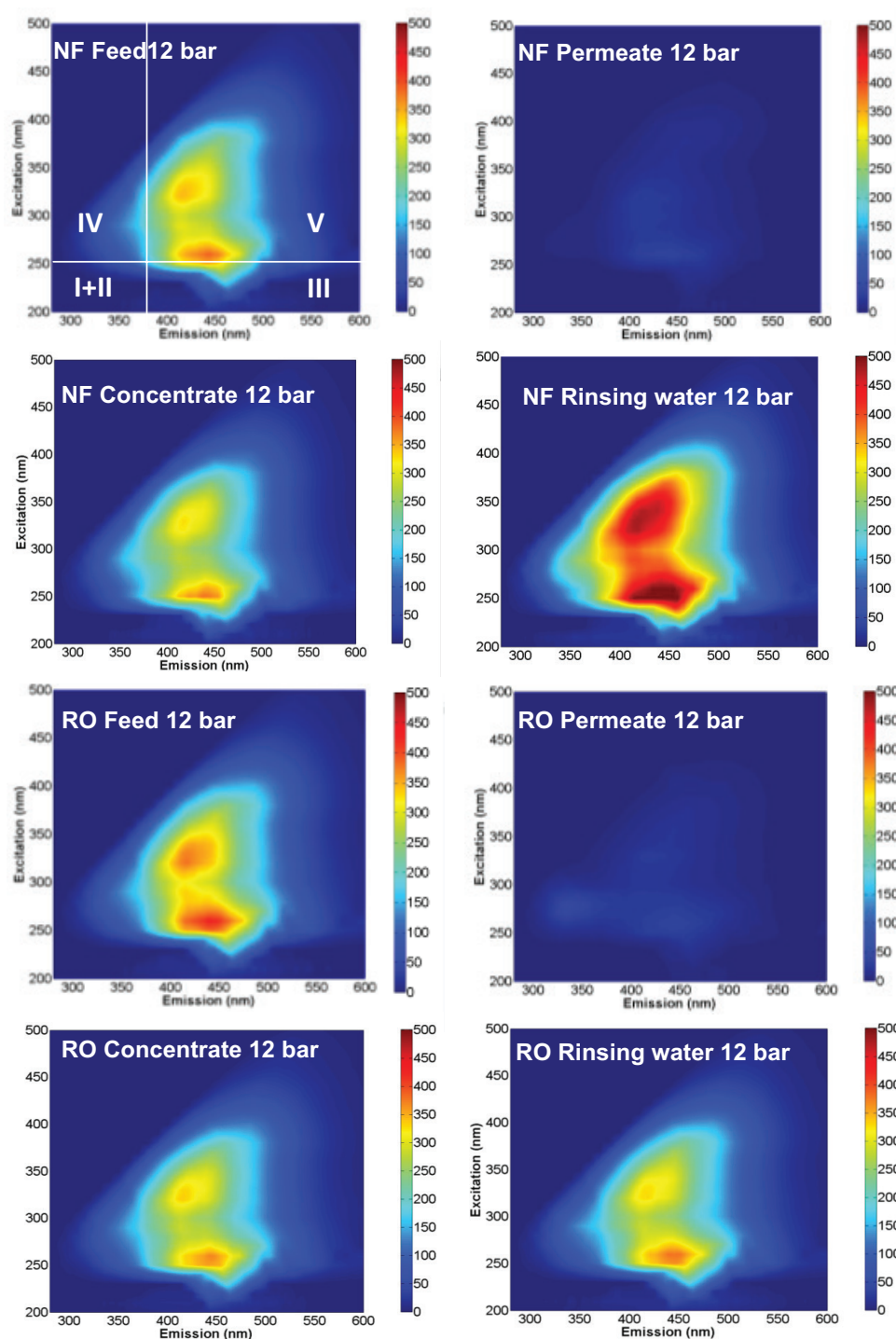


Fig. 3. 3DEEM of NF and RO feeds (4-fold dilution), permeates (no dilution), concentrates (8-fold dilution) and rinsing waters (no dilution).

retained by the NF and RO membranes. This observation also revealed that water rinsing can indeed remove DOM deposits on membrane surface and this was verified by performing a mass balance on the volumes of fluorescence.

Indeed, a mass balance comparison between “volume of fluorescence” and TOC measurements was realized in order to verify whether it could be possible to use the

volumes of fluorescence as a semi-quantitative method. This semi-quantitative prospective approach (detailed in section 2.4) enables sample comparison. The results are displayed in Table 6. It can be seen that less than 25% difference was obtained between the sum of volumes of fluorescence in the collected waters (permeate, rinsing water and concentrate) and that corresponding to the initial feed solution. This

could be acceptable for a semi-quantitative method. TOC mass balances were rather well respected in all the experiments with less than 10% difference. A possible explanation of the previous observations could be that, even if dilutions were performed to get no saturated signal, quenching effects impacted the measurement of the fluorescence intensity. Further research is needed to prove the reliability of such an interesting method.

3.2. Filtration test

Fig. 4 shows the normalized permeate flux J/J_0 decline at 20°C of NF (Fig. 4(a)) or RO (Fig. 4(b)) vs. VCF at 12 and 16 bar for the synthetic mineral effluent (in empty symbols) and for the synthetic effluent containing natural DOM (in filled symbols). The normalized permeate flux corresponds to the ratio between the flux J at 20°C and the initial flux J_0 at 20°C. It enables slight variations of the initial permeabilities between the two membrane coupons to be overcome. In the case of the synthetic mineral effluent, the NF normalized permeate fluxes declined by barely 55% at a VCF of 3, following an almost straight line and were identical. Thus, one could think that the flux decline was mainly due to the increase of osmotic pressure in the feed tank which had probably led to a concentration polarization. In fact, a mass balance of liquid and salts shows the following osmotic pressure evolution (Eq. (6)) with π_f the osmotic pressure in the feed approximately equal to 3 bar and π_c the osmotic pressure in the concentrate which depends on VCF and R . In addition, the driven force will decrease over time due to the increase of osmotic pressure (Eq. (7)):

$$\frac{\pi_c}{\pi_f} = \text{VCF} - (\text{VCF} - 1)(1 - R) \quad (6)$$

$$\begin{aligned} \frac{J}{J_0} &= \frac{\text{Driven Pressure}}{\text{Driven Pressure}_0} = \frac{\text{TMP} - \pi_c}{\text{TMP} - \pi_f} \\ &= \frac{\text{TMP} - \pi_f(\text{VCF} - (\text{VCF} - 1)(1 - R))}{\text{TMP} - \pi_f} \end{aligned} \quad (7)$$

If an average rejection rate R of around 40% is considered in NF (see section 3.1.1) the final corresponding J/J_0 at a VCF of 3 (coming from the basic Darcy's law) is 0.7 instead of 0.55 obtained in reality (Eq. (7)). This means that the flux decline in NF may, finally, not only be due to the increase of

osmotic pressure. The permeate flux was obviously higher at 16 bar than at 12 bar but there was no impact of TMP on the normalized flux declines vs. VCF. In the case of the synthetic effluent containing natural DOM, at 12 bar, the NF normalized permeate flux decline was almost identical to the one without DOM meaning that in these conditions of a maximum VCF of 3, the presence of natural DOM did not impact

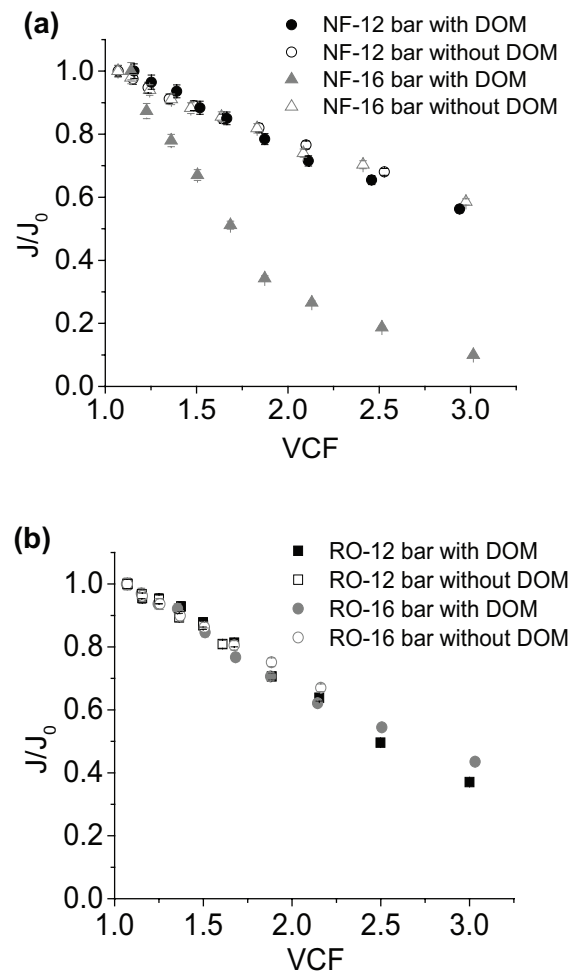


Fig. 4. Normalized permeate flux decline (at 20°C) of NF (a) and RO (b) vs. VCF for the synthetic effluent containing or not DOM at 12 and 16 bar.

Table 6
TOC and volume of fluorescence mass balances

Experiment	Feed	Collected waters	Difference from initial (%)	
NF 12 bar	Volume of fluorescence (arbitrary unit)	6,706	7,962	+19
	TOC (mg)	2.8	2.9	+3 ± 7
NF 16 bar	Volume of fluorescence (arbitrary)	5,975	7,445	+25
	TOC (mg)	3.2	3.0	-6 ± 5
RO 12 bar	Volume of fluorescence (arbitrary)	6,427	6,643	+3
	TOC (mg)	3.0	2.8	-9 ± 5
RO 16 bar	Volume of fluorescence (arbitrary)	5,799	6,698	+15
	TOC (mg)	3.1	3.0	-2 ± 6

the behavior of the flux decline. On the contrary, at 16 bar, the presence of natural DOM increased the flux decline considerably (decline of 90% at VCF of 3) meaning that organic fouling may have occurred. At 16 bar, the potential cake layer may be more compressed, potentially reducing its permeability compared with the filtration at 12 bar.

For both effluents and both TMPs even at 16 bar, the RO normalized flux declines were almost identical to drawing a straight line (decline of 60% at VCF of 3), meaning that the RO flux decline was only due to the increase of osmotic pressure in the feed tank and probably the concentration polarization. This was verified using Eq. (6).

The final normalized flux in RO was naturally lower: around 0.4 (0.4 with Eq. (6)) than the final normalized flux in NF: around 0.55 (0.7 with Eq. (6)) as the salt retention in RO is higher (90% vs. 40%, see section 3.1.1) thus increasing the osmotic pressure in the feed tank. RO flux decline also seems less sensitive to the presence of DOM than NF at 16 bar. One possible explanation could be that the effective pressure ($TMP - \Delta\pi$) in NF was actually higher than in RO because of the very different retention rate (at 16 bar, the effective pressure in NF was 13.8 bar instead of 12.1 bar in RO). This higher effective pressure could have increased the compressibility of the possible cake layer thus decreasing the permeability.

Fig. 5 presents the pure water permeability recoveries after water rinsing and after chemical cleaning. The average value of NF permeability was 10.6 ± 0.2 L/h/m²/bar and the average value of RO permeability was 2.9 ± 0.2 L/h/m²/bar. Taking into account the uncertainty of measurement (which was quite high due to an error of ± 0.1 bar in the pressure sensor), for all the experiments, it could be considered that the permeability was almost fully recovered after simple water rinsing. It would mean that if fouling occurred during filtration, it was almost completely reversible by water rinsing. Even for the NF experiment at 16 bar, the organic fouling seemed reversible. Chemical cleaning did not seem necessary for these short-term experiments showing that fouling was reversible. These assumptions were confirmed by the membrane autopsies (see section 3.3).

3.3. Understanding of NF and RO membrane fouling by membrane autopsy

3.3.1. FTIR analyses

In section 3.2, it was stated that NF and RO flux declines were mainly due to the rise of osmotic pressure and concentration polarization (due to the increase of salt concentration on the concentrate side) which could possibly generate small local scaling. For NF, another contribution to the flux decline was showed and especially at 16 bar in the presence of natural DOM where a steeper flux decline was observed. In addition, for all cases, the permeability recovery analysis led us to conclude that fouling seemed completely reversible and chemical cleaning seemed unnecessary. However, in section 3.1, it was observed that both NF and RO membranes can retain more than 95% of TOC which was also emphasized by 3DEEM analysis and one could expect that this DOM could contribute more substantially to fouling. This present section aims to better understand the different contributions of inorganics and organics on NF and RO membrane fouling by membrane autopsy analysis.

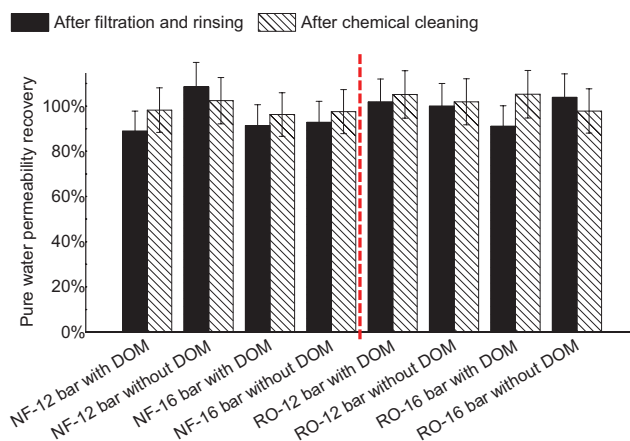


Fig. 5. Analysis of NF and RO pure water permeability recoveries with the synthetic effluent containing or not DOM at 12 and 16 bar.

Fig. 6 shows the ATR-FTIR spectra of the NF and RO membranes before and after filtration, after rinsing and after chemical cleaning at both TMPs. The most common studied wave number range is between 4,000 and 1,300 cm⁻¹ because the absorption peaks mainly correspond to stretching vibration peaks. In the range of 1,300–500 cm⁻¹, the absorption peaks mainly correspond to deformation vibration peaks which are more difficult to analyze. It can be observed that all the unused membranes had the same FTIR absorption spectra corresponding to the FTIR spectra of polyamide [29] as the active layer of both membranes was composed of this material (see Table 3). Indeed, polyamide could be observed as the N–H stretching of amides, which usually occurred in the range of 3,500–3,300, 1,490–1,440 and 850–750 cm⁻¹, and the peak of carbonyl groups (C=O) from primary amides appeared in the range of 1,680–1,630 cm⁻¹.

For all the experiments, the spectra after filtration changed drastically (grey solid line). There was a broad absorption peak between 2,000 and 3,700 cm⁻¹ which may be attributed to C=C stretching in aromatic rings and O–H stretching in alcohols and phenols as well as a sharp absorption peak at 1,600 cm⁻¹ arising from the skeletal vibration of C=C in aromatic rings or C=O stretching in quinone, and a peak around 1,000 cm⁻¹ due to C–O stretching of primary alcohols. These are the characteristics of fulvic acids [30] or humic acids [31] in waters which means that even if the impact of DOM on flux decline was only obvious for the NF experiment at 16 bar, all the membranes after filtration were covered by some DOMs. This type of DOM (fulvic and humic acids) was also in agreement with the 3DEEM analysis (see section 3.1.2). For the NF experiments (Figs. 6(a) and (b)), the FTIR spectra after water rinsing was the same as the unused conditioned membrane, meaning that it could remove all the DOM that may have been deposited on the membrane surface during filtration. After chemical cleaning, the FTIR spectra were also the same, confirming that the chemical cleaning was not really necessary. For the RO experiments, the behavior was the same as for NF at 12 bar (Fig. 6(c)) but a bit different at 16 bar (Fig. 6(d)) where it seems that the water rinsing was not enough to remove the DOM. Only the chemical cleaning could remove

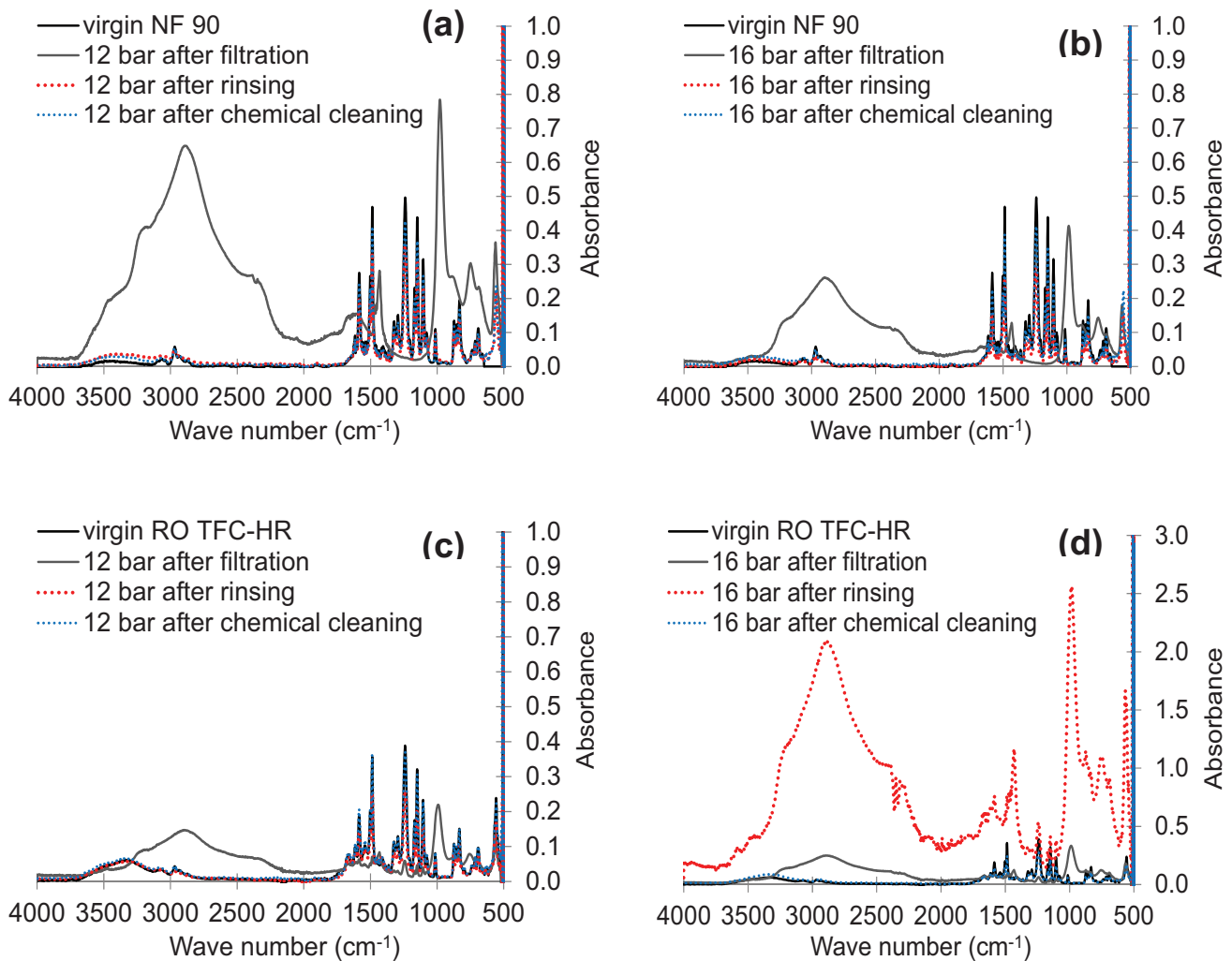


Fig. 6. ATR-FTIR spectra of unused, fouled, rinsed and chemically cleaned membranes for: (a) NF 12 bar, (b) NF 16 bar, (c) RO 12 bar, (d) RO 16 bar.

it and the spectra came back to that of the unused membrane. Therefore, it seemed that fulvic and humic acids were more irreversibly attached to the RO membrane at 16 bar. However, in Fig. 4 in section 3.2, it was shown that NF flux decline at 16 bar was more sensitive to the presence of DOM than RO due to higher cake compressibility. A possible explanation could be that the DOM accumulated on the NF membrane surface was easily removed by water rinsing. On the contrary, in RO, the DOM deposited on the RO membrane surface which did not lead to high flux decline was still visible on the RO surface after water rinsing probably due to more favorable interactions linked to different surface properties between NF and RO membranes (see Table 3).

3.3.2. Contact angle measurements

Contact angle measurements were also performed as a complementary analysis. The results are shown in Table 7. The unused conditioned NF membrane had a contact angle of 42° which is consistent with the literature [32]. The contact angles after filtration followed by water rinsing at both TMPs

Table 7

Contact angles measurements of virgin, fouled, rinsed and chemical cleaned membranes

	Average contact angle	Difference from initial contact angle
Unused conditioned NF membrane	$42 \pm 1^\circ$	
NF after rinsing 12 bar	$28 \pm 1^\circ$	–32%
NF after chemical cleaning 12 bar	$40 \pm 1^\circ$	–4%
NF after rinsing 16 bar	$34 \pm 1^\circ$	–20%
NF after chemical cleaning 16 bar	$41 \pm 1^\circ$	–3%
Unused conditioned RO membrane	$35 \pm 1^\circ$	
RO after rinsing 12 bar	$25 \pm 1^\circ$	–28%
RO after chemical cleaning 12 bar	$33 \pm 1^\circ$	–7%
RO after rinsing 16 bar	$22 \pm 1^\circ$	–38%
RO after chemical cleaning 16 bar	$35 \pm 1^\circ$	–2%

show that the membrane surfaces were more hydrophilic. Some authors found that the hydrophilic fractions were the major component of DOM after conventional activated sludge treatment combined with UF [33] or after the municipal MBR from which the natural DOM came from in this study [28]. However, regarding FTIR analysis, the membrane surface after rinsing was exempt of DOM. Contact angle measurements may therefore indicate the presence of hydrophilic compounds which may be therefore rather inorganic. Indeed, contact angle measurement of the dried membranes after filtration (probably covered by some mineral deposits in addition to DOM) was not possible as the drop was completely spread (0°). The following paragraph about SEM-EDX analysis may confirm this assumption. Finally, the chemical cleaning resulted in measurements of almost the initial value

of the contact angle, proving that this can be useful. The unused conditioned RO membrane had a contact angle of 35° which is also consistent with the literature [34,35]. The same behavior as for NF was observed after filtration followed by water rinsing and after chemical cleaning.

3.3.3. SEM-EDX analysis

Finally, to visualize and quantify possible mineral deposits on the membrane surfaces, SEM-EDX analyses were performed. SEM pictures of the NF membranes are shown in Fig. 7 and the corresponding EDX analysis in Table A1 of supplementary material at 12 bar and Table A2 at 16 bar. The unused NF membrane had a flat homogeneous surface made of C, O and S, the atoms of the polysulfone support layer.

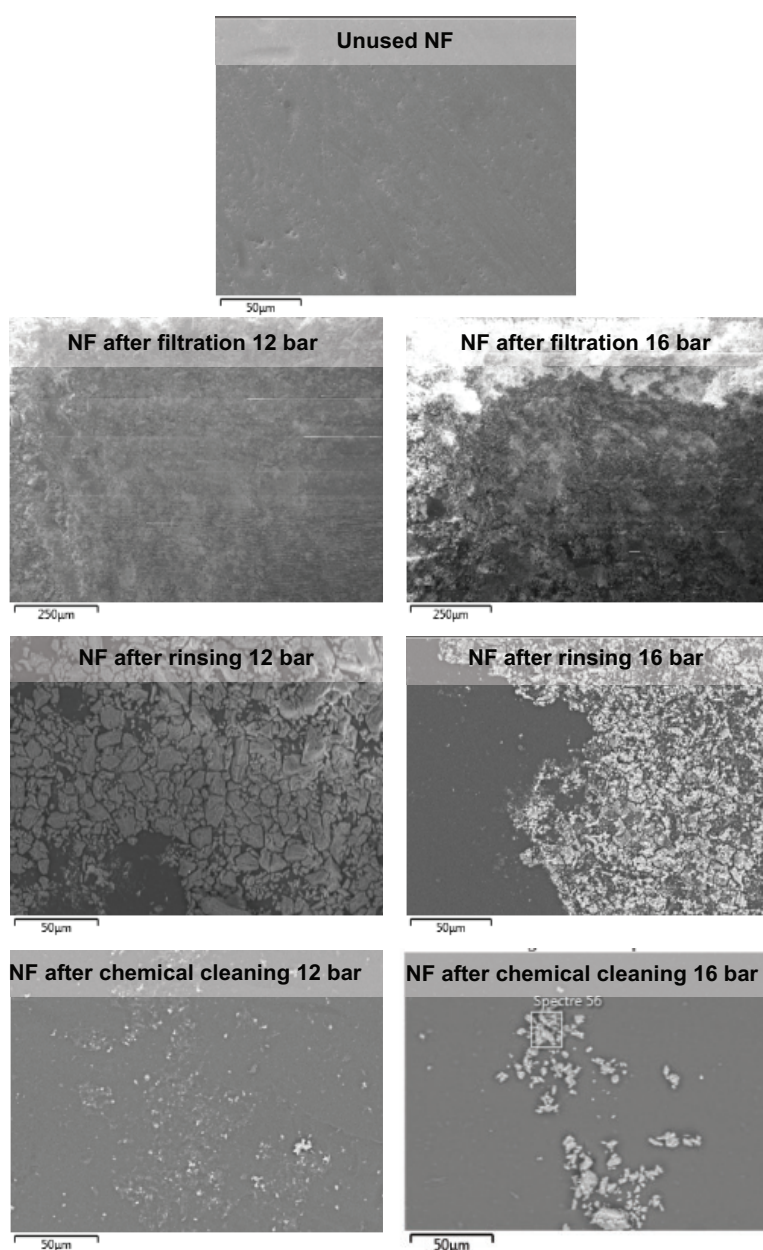


Fig. 7. SEM pictures of unused, fouled, rinsed and chemically cleaned NF membranes.

It seems that N atoms of polyamide filtration layer were not visible. The SEM NF membranes pictures after filtrations at both TMPs were not very clear due to a dense fouling layer (of minerals and organics) which probably saturated the signal. The resulting EDX analysis was thus not very precise but it can be stated that the fouling layer contained C, N, O, Mg and P atoms possibly among others. The SEM pictures of the NF membranes after water rinsing are more informative. It can be seen that there were still mineral deposits on the NF membrane surface. The EDX revealed that in addition to the clean NF membrane surface composition (C, N, S), other atoms which came from the mineral deposits were the following: N, Mg, P, Si, K and Ca. These observations were in agreement with the assumption formulated in section 3.3.2. After chemical cleaning, the SEM pictures revealed that the

NF membrane surfaces were cleaner but some small mineral deposits were still present. The EDX analysis confirmed this observation: the composition was almost the same as the unused membrane: about 50% of C, about 40% of O and about 5% of S plus some other atoms such as N, Mg, P and Ca in smaller concentrations (less than 5%). SEM pictures of the RO membranes are shown in Fig. 8 and the corresponding EDX analysis in Table A3 of supplementary material at 12 bar and Table A4 at 16 bar. The unused RO membrane had a flat homogeneous surface made of C, O, N and Cl atoms which may come from the polyamide filtration layer and S atoms coming from the polysulfone support layer. The RO membranes SEM pictures after filtrations at both TMPs were clearer than the ones of the NF membranes. Small heterogeneous mineral deposits could be seen, composed of C, N, O,

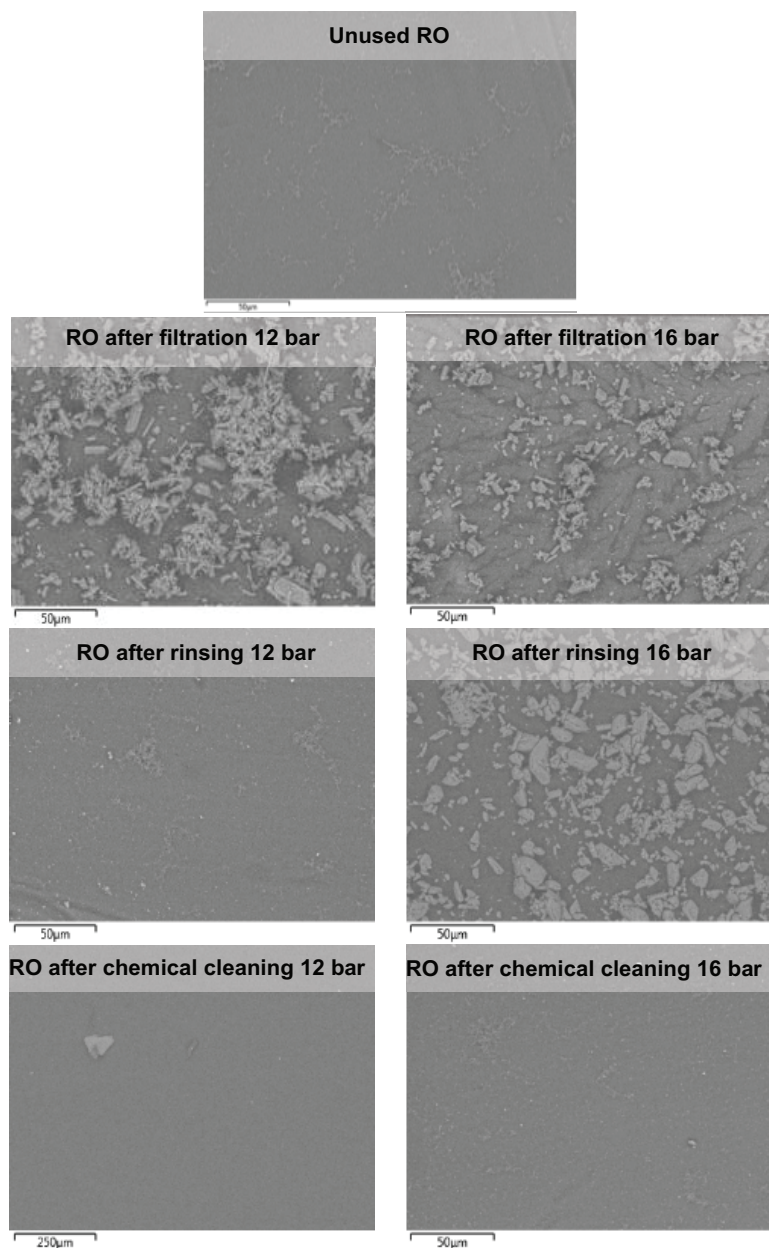


Fig. 8. SEM pictures of unused, fouled, rinsed and chemically cleaned RO membranes.

Na, Mg, Si, P, S, Cl, K and Ca atoms. P and Mg atoms were predominant and represented more than 10% of the total. The pictures and SEM analysis of the RO membranes after water rinsing showed that there was a difference between the TMPs. At 12 bar, the surface was rather clean which was confirmed by the EDX analysis. This latter was very similar to that of the unused membrane with less than 0.2% of Cl, Si or Mg residues. Conversely, at 16 bar, the surface was still covered by some mineral deposits composed of Mg, Si, P, S, K and Ca in the same proportions as after filtration. The water rinsing only seemed to remove Na and Cl atoms. The previous FTIR analysis also showed that the water rinsing was not effective in removing the humic and fulvic acids on the RO surface after filtration at 16 bar. After chemical cleaning, the SEM pictures revealed that the RO membrane surfaces were almost as clean as the unused membranes. The EDX analysis confirmed this observation: the composition was the same as the virgin membrane: 51.6% of C, 1.1% of N, 43.2% of O, 3.8% of S and 0.2% of Cl. Chemical cleaning seemed more efficient in completely removing mineral deposits on the RO membrane than on the NF membrane whereas the concentration of NaOH and HCl was 10 times lower for the RO chemical cleaning than for the NF chemical cleaning. A possible reason could be the lower RO membrane roughness (Table 3) than that of the NF membrane, thus reducing the potential of nucleation before scaling. Moreover, the effective pressure (TMP- $\Delta\pi$) was lower in RO than in NF.

4. Summary and conclusion

The present study of the performances of NF and RO as complementary treatments after MBR for source-separated urine treatment and reuse with a synthetic effluent containing natural DOM, led to specific macroscale and macroscale

results which can be summarized in Tables 8 and 9, respectively.

To fully understand the short-term fouling behavior, several cross analyses were necessary. On the macroscale, it was supposed that for NF and RO, the flux decline was mainly due to the rise of osmotic pressure except for NF and especially at 16 bar where DOM generated a higher flux decline. DOM was almost completely removed from the effluent by NF and RO at any TMP. And, in all cases, the analysis of the permeabilities after water rinsing and after chemical cleaning showed that possible fouling seemed to be completely removed by water rinsing. On the microscale, it was seen that some DOM was present on the membrane surface after filtration for all cases and even after water rinsing for RO at 16 bar (but without impact on flux decline). Chemical cleaning can completely remove DOM. Furthermore, even if RO presents higher mineral (ions) rejection rates, it was observed on the microscale that more minerals were present on the NF surface, even after water rinsing (except for RO at 16 bar). After chemical cleaning, a few minerals were still only present on the NF membranes.

Consequently, macroscale observations are apparently not always consistent with microscale observations. In this present case, several filtration cycles could have possibly shown the impact on the macroscale of the remaining fouling observed on the microscale.

For source-separated urine treatment and water reuse, RO seems more efficient in terms of water quality and less prone to fouling at low TMP than NF, confirming the RO relevance for this application. However, in order to fully comply with WHO guidelines, adjustment of MBR treatment conditions is needed to remove nitrogen based compounds (NO_2^- , NO_3^- and NH_4^+) more efficiently as RO can only remove 80% of nitrogen compounds. To complete this work, experiments with real source-separated urine will be performed.

Table 8
Summary of macroscale results

Experimental conditions	Flux decline	Permeability after filtration + rinsing	Permeability after chemical cleaning	DOM rejection	Monovalent ions rejection	Tri- or divalent ions rejection
NF 12 bar	+	=	=	+++	-	+
NF 16 bar	+++	=	=	+++	-	++
RO 12 bar	+	=	=	+++	++	++
RO 16 bar	+	=	=	+++	++	+++

Table 9
Summary of microscale results

Experimental conditions	DOM on membrane after filtration	DOM on membrane after rinsing	DOM on membrane after chemical cleaning	Minerals on membrane after filtration	Minerals on membrane after rinsing	Minerals on membrane after chemical cleaning
NF 12 bar	+++	-	-	+++	++	+
NF 16 bar	+++	-	-	+++	++	+
RO 12 bar	++	-	-	++	+	-
RO 16 bar	++	++	-	++	++	-

Acknowledgments

The authors would like to thank BPI France, through Carbiosep project (FUI -AAP20) carried by BFG Environmental Technologies for its financial support. Special thanks are addressed to Yves-Marie Legrand for his help for the development of 3DEEM techniques and Valerie Bonniol for the ion chromatography analysis.

Symbols

C_f	—	Salt concentration in the feed
C_p	—	Salt concentration in the permeate
I^p	—	Fluorescence intensity
$L_{p_{20^\circ\text{C}}}$	—	Solvent permeability at 20°C
$L_{p_{T^\circ\text{C}}}$	—	Solvent permeability at T°C
R	—	Apparent rejection rate
V_0	—	Initial volume of the solution
V_p	—	Volume of collected permeate
\sqrt{VCF}	—	Volumetric concentration factor
Y	—	Recovery rate
$\Delta\lambda_{em}$	—	Emission wavelength interval
$\Delta\lambda_{ex}$	—	Excitation wavelength interval
$\mu_{20^\circ\text{C}}$	—	Dynamic viscosity at 20°C
$\mu_{T^\circ\text{C}}$	—	Dynamic viscosity at T°C
π_f	—	Osmotic pressure of the feed solution
π_c	—	Osmotic pressure of the concentrate
Φ	—	Volume of fluorescence

References

- [1] S. Eslamian, Ed., *Urban Water Reuse Handbook*, CRC Press, Taylor & Francis Group, Boca Raton, USA, 2016.
- [2] M. El-Ahsry, B. Zeitoon, N. Saab, *Arab Environment, Water, Sustainable Management of a Scarce Resource: 2010 Report of the Arab Forum for Environment and Development (AFED)*, Arab Forum for Environment and Development (AFED), Beirut, 2010.
- [3] T. Larsen, W. Gujer, Separate management of anthropogenic nutrient solutions (human urine), *Water Sci. Technol.*, 34 (1996) 87–94.
- [4] A.B. Bisinella de Faria, M. Spérandio, A. Ahmadi, L. Tiruta-Barna, Evaluation of new alternatives in wastewater treatment plants based on dynamic modelling and life cycle assessment (DM-LCA), *Water Res.*, 84 (2015) 99–111.
- [5] W. Pronk, H. Palmquist, M. Biebow, M. Boller, Nanofiltration for the separation of pharmaceuticals from nutrients in source-separated urine, *Water Res.*, 40 (2006) 1405–1412.
- [6] M. Maurer, W. Pronk, T.A. Larsen, Treatment processes for source-separated urine, *Water Res.*, 40 (2006) 3151–3166.
- [7] M. Aslam, A. Charfi, G. Lesage, M. Heran, J. Kim, Membrane bioreactors for wastewater treatment: a review of mechanical cleaning by scouring agents to control membrane fouling, *Chem. Eng. J.*, 307 (2017) 897–913.
- [8] S. Judd, C. Judd, Eds., *The MBR Book: Principles and Applications of Membrane Bioreactors for Water and Wastewater Treatment*, 2nd ed., Elsevier/BH Butterworth-Heinemann, Amsterdam, 2011.
- [9] K.M. Udert, T.A. Larsen, W. Gujer, Fate of major compounds in source-separated urine, *Water Sci. Technol.*, 54 (2006) 413–420.
- [10] S.-P. Sun, C.P. i Nàcher, B. Merkey, Q. Zhou, S.-Q. Xia, D.-H. Yang, J.-H. Sun, B.F. Smets, Effective Biological Nitrogen Removal Treatment Processes for Domestic Wastewaters with Low C/N Ratios: A Review, *Environ. Eng. Sci.*, 27 (2010) 111–126.
- [11] J. Lin, P. Zhang, G. Li, J. Yin, J. Li, X. Zhao, Effect of COD/N ratio on nitrogen removal in a membrane-aerated biofilm reactor, *Int. Biodeterior. Biodegrad.*, 113 (2016) 74–79.
- [12] Q. Meng, F. Yang, L. Liu, F. Meng, Effects of COD/N ratio and DO concentration on simultaneous nitrification and denitrification in an airlift internal circulation membrane bioreactor, *J. Environ. Sci.*, 20 (2008) 933–939.
- [13] G. Ruiz, D. Jeison, R. Chamy, Nitrification with high nitrite accumulation for the treatment of wastewater with high ammonia concentration, *Water Res.*, 37 (2003) 1371–1377.
- [14] V.M. Vadivelu, J. Keller, Z. Yuan, Free ammonia and free nitrous acid inhibition on the anabolic and catabolic processes of *Nitrosomonas* and *Nitrobacter*, *Water Sci. Technol.*, 56 (2007) 89.
- [15] Y.C. Woo, J.J. Lee, W.-G. Shim, H.K. Shon, L.D. Tijing, M. Yao, H.-S. Kim, Effect of powdered activated carbon on integrated submerged membrane bioreactor–nanofiltration process for wastewater reclamation, *Bioresour. Technol.*, 210 (2016) 18–25.
- [16] C. Kappel, A.J.B. Kemperman, H. Temmink, A. Zwijnenburg, H.H.M. Rijnaarts, K. Nijmeijer, Impacts of NF concentrate recirculation on membrane performance in an integrated MBR and NF membrane process for wastewater treatment, *J. Membr. Sci.*, 453 (2014) 359–368.
- [17] M. Jacob, C. Guigui, C. Cabassud, H. Darras, G. Lavison, L. Moulin, Performances of RO and NF processes for wastewater reuse: tertiary treatment after a conventional activated sludge or a membrane bioreactor, *Desalination*, 250 (2010) 833–839.
- [18] S. Lee, R.M. Lueptow, Reverse osmosis filtration for space mission wastewater: membrane properties and operating conditions, *J. Membr. Sci.*, 182 (2001) 77–90.
- [19] K.M. Udert, M. Wächter, Complete nutrient recovery from source-separated urine by nitrification and distillation, *Water Res.*, 46 (2012) 453–464.
- [20] S. Carretier, G. Lesage, A. Grasmick, M. Heran, Water and nutrients recovering from livestock manure by membrane processes, *Can. J. Chem. Eng.*, 93 (2015) 225–233.
- [21] A. Azais, J. Mendret, S. Gassara, E. Petit, A. Deratani, S. Brosillon, Nanofiltration for wastewater reuse: counteractive effects of fouling and matrice on the rejection of pharmaceutical active compounds, *Sep. Purif. Technol.*, 133 (2014) 313–327.
- [22] S.S. Deshmukh, A.E. Childress, Zeta potential of commercial RO membranes: influence of source water type and chemistry, *Desalination*, 140 (2001) 87–95.
- [23] W. Chen, P. Westerhoff, J.A. Leenheer, K. Booksh, Fluorescence excitation–emission matrix regional integration to quantify spectra for dissolved organic matter, *Environ. Sci. Technol.*, 37 (2003) 5701–5710.
- [24] J.V. Nicolini, C.P. Borges, H.C. Ferraz, Selective rejection of ions and correlation with surface properties of nanofiltration membranes, *Sep. Purif. Technol.*, 171 (2016) 238–247.
- [25] L. Paugam, C.K. Diawara, J.P. Schlumpf, P. Jaouen, F. Quéméneur, Transfer of monovalent anions and nitrates especially through nanofiltration membranes in brackish water conditions, *Sep. Purif. Technol.*, 40 (2004) 237–242.
- [26] World Health Organization, *Wastewater Use in Agriculture*, 3rd ed., World Health Organization, Geneva, 2006.
- [27] World Health Organization, *Guidelines for Drinking-Water Quality*, 2011.
- [28] C. Jacquin, G. Lesage, J. Traber, W. Pronk, M. Heran, Three-dimensional excitation and emission matrix fluorescence (3DEEM) for quick and pseudo-quantitative determination of protein- and humic-like substances in full-scale membrane bioreactor (MBR), *Water Res.*, 118 (2017) 82–92.
- [29] M.B.M.Y. Ang, Y.-L. Ji, S.-H. Huang, H.-A. Tsai, W.-S. Hung, C.-C. Hu, K.-R. Lee, J.-Y. Lai, Incorporation of carboxylic monoamines into thin-film composite polyamide membranes to enhance nanofiltration performance, *J. Membr. Sci.*, 539 (2017) 52–64.
- [30] Y. Dang, Y. Lei, Z. Liu, Y. Xue, D. Sun, L.-Y. Wang, D.E. Holmes, Impact of fulvic acids on bio-methanogenic treatment of municipal solid waste incineration leachate, *Water Res.*, 106 (2016) 71–78.
- [31] S. Zhang, L. Yuan, W. Li, Z. Lin, Y. Li, S. Hu, B. Zhao, Characterization of pH-fractionated humic acids derived from Chinese weathered coal, *Chemosphere*, 166 (2017) 334–342.

- [32] A.A. Alturki, N. Tadkaew, J.A. McDonald, S.J. Khan, W.E. Price, L.D. Nghiem, Combining MBR and NF/RO membrane filtration for the removal of trace organics in indirect potable water reuse applications, *J. Membr. Sci.*, 365 (2010) 206–215.
- [33] H.K. Shon, S. Vigneswaran, I.S. Kim, J. Cho, H.H. Ngo, Fouling of ultrafiltration membrane by effluent organic matter: a detailed characterization using different organic fractions in wastewater, *J. Membr. Sci.*, 278 (2006) 232–238.
- [34] B.C. Ricci, C.D. Ferreira, L.S. Marques, S.S. Martins, B.G. Reis, M.C.S. Amaral, Assessment of the chemical stability of nanofiltration and reverse osmosis membranes employed in treatment of acid gold mining effluent, *Sep. Purif. Technol.*, 174 (2017) 301–311.
- [35] P. Xu, J.E. Drewes, Viability of nanofiltration and ultra-low pressure reverse osmosis membranes for multi-beneficial use of methane produced water, *Sep. Purif. Technol.*, 52 (2006) 67–76.

Supplementary material

Table A1
EDX element analysis in average weight % for unused, fouled, rinsed and chemically cleaned NF at 12 bar

Element	Unused conditioned NF	NF after filtration	NF after rinsing	NF after chemical cleaning
C	52.9 ± 0.1	38.9 ± 5.8	18.0 ± 3.4	44.0 ± 7.9
N	–	5.7 ± 1.2	0.5 ± 0.2	0.1 ± 0.1
O	42.3 ± 0.02	48.2 ± 1.9	47.5 ± 0.8	43.7 ± 1.1
Mg	–	5.1 ± 2.0	13.0 ± 1.1	3.5 ± 3.2
Si	–	–	1.0 ± 0.0	0.1 ± 0.1
P	–	2.0 ± 0.8	17.4 ± 1.6	4.6 ± 4.2
S	4.7 ± 0.04	–	0.8 ± 0.3	3.9 ± 0.9
K	–	–	0.4 ± 0.01	0.1 ± 0.1
Ca	–	–	1.5 ± 0.4	0.1 ± 0.1
Total	100	100	100	100

Table A2
EDX element analysis in average weight % for unused, fouled, rinsed and chemically cleaned NF at 16 bar

Element	Unused conditioned NF	NF after filtration	NF after rinsing	NF after chemical cleaning
C	52.9 ± 0.1	26.4	32.2 ± 10.7	52.2 ± 0.7
N	–	8.3	–	–
O	42.3 ± 0.02	52.3	42.4 ± 0.1	42.3 ± 0.1
Mg	–	9.1	1.2 ± 0.6	–
Si	–	–	0.2 ± 0.1	0.3 ± 0.2
P	–	3.9	7.9 ± 4.2	0.0 ± 0.1
S	4.7 ± 0.0	–	3.1 ± 1.0	4.6 ± 0.1
Ca	–	–	13.1 ± 6.6	0.6 ± 0.7
Total	100	100	100	100

Table A3
EDX element analysis in average weight % for unused, fouled, rinsed and chemically cleaned RO at 12 bar

Element	Unused conditioned RO	RO after filtration	RO after rinsing	RO after chemical cleaning
C	51.7 ± 0.3	25.3 ± 17.2	51.3 ± 0.2	51.6 ± 0.4
N	1.1 ± 0.1	1.0 ± 0.6	1.1 ± 0.05	1.1 ± 0.05
O	43.2 ± 0.2	46.8 ± 3.5	43.3 ± 0.1	43.2 ± 0.2
Na	–	0.5 ± 0.5	–	–
Mg	–	9.8 ± 6.2	0.03 ± 0.02	–
Si	–	0.1 ± 0.1	0.04 ± 0.03	–
P	–	14.0 ± 9.5	–	–
S	3.8 ± 0.05	1.4 ± 1.4	4.0 ± 0.02	3.9 ± 0.2
Cl	0.2 ± 0.01	0.6 ± 0.6	0.2 ± 0.0	0.2 ± 0.01
K	–	0.3 ± 0.03	–	–
Ca	–	0.3 ± 0.2	–	–
Total	100	100	100	100

Table A4
EDX element analysis in average weight % for unused, fouled, rinsed and chemically cleaned RO at 16 bar

Element	Unused conditioned RO	RO after filtration	RO after rinsing	RO after chemical cleaning
C	51.7 ± 0.3	11.9 ± 2.1	11.5 ± 3.3	51.6 ± 0.4
N	1.1 ± 0.1	1.1 ± 0.3	1.1 ± 0.2	1.1 ± 0.05
O	43.2 ± 0.2	49.0 ± 0.3	49.2 ± 0.5	43.2 ± 0.2
Na	–	0.2 ± 0.2	–	–
Mg	–	15.7 ± 1.0	15.7 ± 1.1	–
Si	–	0.3 ± 0.1	0.3 ± 0.03	–
P	–	20.6 ± 1.4	21.2 ± 2.3	–
S	3.8 ± 0.05	0.2 ± 0.1	0.1 ± 0.2	3.9 ± 0.2
Cl	0.2 ± 0.01	0.3 ± 0.2	–	0.2 ± 0.01
K	–	0.4 ± 0.1	0.3 ± 0.1	–
Ca	–	0.3 ± 0.1	0.6 ± 0.2	–
Total	100	100	100	100